Thin-Walled Structures 122 (2018) 359–370

Contents lists available at ScienceDirect

Thin-Walled Structures

journal homepage: www.elsevier.com/locate/tws

Full length article

Seismic response of CFS shear walls sheathed with nailed gypsum panels: Numerical modelling

Luigi Fiorino*, Sarmad Shakeel, Vincenzo Macillo, Raffaele Landolfo

Department of Structures for Engineering and Architecture, University of Naples "Federico II", Naples, Italy

ARTICLE INFO

Keywords:
Cold-formed steel
Sheathed-braced systems
Gypsum-based panels
Nailed connections
Hysteretic behaviour
Non-linear model
Finite element model
Simplified truss model

ABSTRACT

Building codes around the globe are in a transition to update their design guidelines to meet the objectives of performance based seismic design (PBSD). The fulfilment of the objectives of PBSD requires number of collapse simulations of a building equipped with certain type of seismic force resistant system. Numerical models with an ability to simulate post-peak deteriorating behaviour are essential for these collapse simulations. A European research project named ELISSA was carried out in recent years, to better understand the seismic behaviour of cold-formed steel shear walls sheathed with nailed gypsum based panels through experimental and numerical studies. Within the framework of project, numerical models were developed for single shear walls with an ability to simulate their nonlinear hysteretic behaviour and possessing the capability of being used in the collapse simulations of complete building models for meeting the PBSD objectives. These models are the focus of the study presented herein. Three types of models are presented, which differ with each other in terms of complexity, type of experimental results used in their calibration and the ability to simulate nonlinear monotonic or cyclic lateral static behaviour.

1. Introduction

High structural, technological and environmental performance of lightweight steel constructions has presented them as a better alternative for low to medium rise buildings located in seismic areas. Cold-Formed Steel (CFS) members are mainly used as the structural elements in these types of constructions. Shear walls, made of flat sheets of steel, wood, gypsum or fibreboard based panels attached to the CFS frame through screw or nail fastener systems, is one of the techniques to provide the seismic resistance in lightweight steel constructions. It has been evident from the previous research on these type of walls [1–4], that the interaction between sheathing panels and CFS frame represents the most significant nonlinear behaviour and strongly influences the lateral response of walls. Pin-connected horizontal and vertical elements of CFS frame cause it to deform into a parallelogram under the in-plane shear loads. The sheathing itself behaves as a rigid element and can only undergo rotation and translations. Inconsistent deformation of the steel frame into parallelogram and rigid body deformation of the sheathing produces tilting or bearing deformations in sheathing panel-to-steel frame connections, which is the key energy dissipation mechanism.

Regardless of the several benefits offered by lightweight steel construction in seismic areas, a lack of confidence exists in the European construction sector on use of this system, mainly due to the absence of proper design guidelines [5] and the existence of the very few applications [6,7]. In this regard, a European research project named ELISSA (Energy Efficient LIghtweight-Sustainable-SAfe-Steel Construction) [8] was conducted among different universities, research centres and material manufactures across Europe to promote the use of CFS systems. In particular, University of Naples Federico II, Italy, provided the seismic behaviour assessments of the wall constructions through several experimental and numerical studies. From structural point of view, the walls were sheathed-braced CFS shear walls made with impact resistant gypsum board panels (Diamant-X by Knauf) attached to the CFS frame through ballistic nails. Profiles in CFS frame were joined together using clinching techniques. The use of these connecting techniques in walls led to a more efficient level of prefabrication, thanks to their fast execution speed.

In order to evaluate the seismic behaviour of shear walls, a case study of a building representing a real-world application of lightweight steel construction was developed in the project. More details about the case study are provided in [9]. The performance of shear walls was investigated by means of experimental tests organized on three subsequent scale levels: micro-scale, meso-scale and macro-scale. At micro-scale level, monotonic and cyclic tests were conducted on sheathing connections made using ballistic nails [10]. Meso-scale tests included

* Corresponding author.
E-mail addresses: lfiorino@unina.it (L. Fiorino), sarmad.shakeel@unina.it (S. Shakeel), vincenzo.macillo@unina.it (V. Macillo), landolfo@unina.it (R. Landolfo).

http://dx.doi.org/10.1016/j.tws.2017.10.028
Received 27 April 2017; Received in revised form 21 September 2017; Accepted 16 October 2017
Available online 13 November 2017

monotonic and cyclic tests on full-scale shear walls. Finally, macro-scale shaking table tests of complete two storey building [9] were conducted in order to evaluate its global seismic response.

Nowadays, modern earthquake standards are following a trend to integrate the performance based seismic design (PBSD) approaches in order to achieve a more rational design [11]. Development of PBSD requires to achieve a level of damage in structure, which can be simulated through nonlinear dynamic analysis of computational models having the capability to represent the deteriorating structural behaviour. Therefore, along with the experimental studies, nonlinear numerical models were also developed for the specimens tested at all three stages. Additionally, numerical modelling at each scale were also utilized to predict the response of subsequent experimental phases. This paper explains the three different approaches, which are adopted in the study presented herein for the development of numerical models of CFS shear walls sheathed with nailed gypsum boards to simulate their monotonic and cyclic response (meso-scale level). In the first approach, the experimental results of micro-scale sheathing connection tests were used to predict the monotonic or cyclic envelope response of shear walls using a detailed finite element (FE) model. In the second approach, an equivalent truss model was developed to simulate the wall hysteretic response using the experimental results of the meso-scale cyclic tests on shear walls. In the third approach, a procedure for simulating the cyclic response of shear walls through a unified FE-truss model was proposed, which only relies on test results on individual sheathing connection assemblies and is simplified enough to be used with complete building models. The experimental results used in the development of these models are presented in the companion paper [12].

2. Previous researches on the numerical modelling

The dynamic behaviour of CFS-sheathing-braced shear walls is characterized by a remarkable nonlinear response with a strong pinching of the hysteresis loops and degradation of the strength and stiffness in subsequent loops. In past, various researchers proposed numerical models to simulate this type of response. They can be broadly categorized into equivalent truss, equivalent shell and detailed finite element (FE) models based on the approach used in their development and the resulting inherent complexity. An equivalent truss model [13–18] relies on equivalent nonlinear truss elements or linear truss elements combined with nonlinear springs to simulate the behaviour of a shear wall. A shell model [19] uses shell elements with equivalent mechanical and physical properties, which are representative of complete wall behaviour, to simulate the nonlinear behaviour of a shear wall. Detailed FE models [20–24] follow a more realistic approach by simulating the nonlinear response of a complete shear wall through modelling of main structural elements, including all individual sheathing connections, which are the main energy dissipating mechanism in walls. Following paragraphs highlight the modelling approach used in different studies for developing the numerical models for CFS-sheathing braced shear walls.

Fülöp and Dubina [13] developed an equivalent truss model using DRAIN-3DX [25] software for CFS shear walls sheathed with corrugated steel sheets or OSB panels. They represented the nonlinear behaviour of the shear wall through pair of diagonal trusses having a fibre-hinge accommodating the desired hysteretic behaviour, which was calibrated using experimental results [26].

A similar modelling approach was followed by Shamim and Rogers [14] for CFS sheathed shear walls in OpenSees [27] software. They used nonlinear truss elements in a X configuration paired with an elastic wall frame, to represent the wall response under dynamic loading. In particular, they used *Pinching4 material* [28] for nonlinear truss elements, which possess the ability to simulate the pinched hysteretic response typical of CFS shear walls.

Very recently, North American cold formed research groups finished a project short named as CFS-NEES [29] aimed at better understanding of seismic behaviour and the improved design of CFS structures. In the project, a 2 storey CFS sheathed braced building was tested on shake table. Leng at al [15] developed the computational models for the tested structure. The models developed for shear walls were similar to the one developed by Shamim and Rogers [14]. In addition to using piching4 material for truss elements, they also tried to use an Elastic Perfectly Plastic material, which failed to provide better results than pinching4 material model. Moreover, for modelling the response of complete building they divided the shear walls in into sub panels. The lateral stiffness of each individual sub panel was modelled by pair of two diagonal truss elements having a picnhing4 material.

Kechidi and Bourahla [16] presented an equivalent truss model developed in Opensees [27] software for wood and steel sheathed CFS shear walls. They used a pair of rigid truss elements in a X configuration with an equivalent non-linear *Zero Length element* in the mid of truss elements having user-defined material to represent the wall behaviour. Additionally, they also developed a uniaxial material, which uses only the physical and mechanical characteristics of the wall as input to simulate the wall hysteretic response. The criteria governing the hysteretic behaviour of the uniaxial material was selected based on relevant experimental results.

Bourahla et al. [17] presented a simple model to account for the overall lateral stiffness and strength of the shear walls in the complete building models in SAP2000 software [30]. Model used a nonlinear equivalent shear link having a pivot hysteretic model connected to rigid triangular shell elements. They achieved a quite good match in terms of comparison of dynamic properties of numerical model of complete building with the results obtained from its ambient vibration testing.

The nonlinear hysteretic response of shear walls can also be represented by a set of differential equations which define the material rule for a nonlinear spring representing the behaviour of the shear wall. One such model was presented by Nithyadharan and Kalyanaraman [18], which used Bouc-Wen-Baber-Noori [31] smooth differential model in order to simulate the response of CFS shear walls braced with calcium silicate panels.

Martinez et al. [19] followed a more simplified modelling approach by simulating the behaviour of wood-sheathed CFS shear walls using an equivalent orthotropic shell elements in SAP2000 software [30]. The equivalent properties of shell elements were adjusted to account for the global behaviour of the shear wall.

Buonopane et al. [20] presented a detailed finite element model developed in OpenSees software [27] representing the main energy dissipating component (sheathing connections) in wood sheathed CFS shear walls through radially-symmetric nonlinear spring elements placed at each sheathing connection location. Rigid behaviour of OSB or gypsum sheathing panels was modelled through the *rigid diaphragm*, whereas the CFS frame was modelled using *elastic beam column elements*. *Pinching4 material* [28] was used for the nonlinear spring elements, which was calibrated based on the experimental results of sheathing connection tests.

Niari et al. [21] developed finite element models for steel-sheathed CFS shear walls in ABAQUS software [32] for simulating their monotonic response. *S4R shell element* with reduced integration was used to model the CFS frame and sheathing, whereas steel sheet-to-profile connections were modelled with *mesh independent fasteners*, which were calibrated on the basis of experimental results on individual connection tests.

Zhou et al. [22] developed a detailed finite element model for wood-sheathed CFS shear walls in ANSYS software [33] and compared their performance against the results of monotonic tests on shear walls. They modelled the frame and sheathing with the *Shell181 element* and used coupling methods to handle the panel-to-steel profile connections that allowed only rotation in connections, restricting any translation.

Telue and Mahendran [23] also developed detailed finite element models for wood-sheathed CFS shear walls for the evaluation of their monotonic response using ABAQUS [32] software. They used ABAQUS

S4R5 shell to model the CFS frame and *B31 beam elements* to model sheathing connections.

Ding [24] at Virginia Tech developed a user element (UEL) for sheathing connections in ABAQUS based on the pinching4 material available in OpenSees. Then using the developed UEL for connections, a high-fidelity model of CFS OSB sheathed shear was developed. Frame and sheathing were both modelled as shell elements. Performance of models was quite good under the monotonic loading while for cycling loading models experienced divergence in the solution. In order to overcome this, they locked the direction of faster deformation once it enters the plastic zone, which lead to the convergence of solution.

To sum up, the models explained earlier are able to predict the in-plane static and dynamic response of CFS-sheathed shear walls with good accuracy. Models developed following an equivalent truss or shell approach [13,14,18,19] use the shear wall test results for the calibration purposes. Although these equivalent models require full scale wall test data as input, their modelling simplicity allows to use them in simulating the nonlinear dynamic response of whole buildings [20,21,34,35] under given ground motions. On the other hand, detailed FE models allow the simulation of the shear wall response using the results of sheathing connection tests, but due to their high computational complexity, they cannot be used for whole building modelling. In order to fill these gaps, a proposal, which only uses sheathing connection test results as inputs and allows to simulate the nonlinear dynamic response of whole buildings, could be very useful and is the main goal of this study. In order to achieve this goal, numerical models are developed following three different approaches, as explained earlier in the introduction.

In the first approach, detailed FE models are developed using SAP2000 software framework. Detailed FE models have already been developed by some researchers [20–24] using other software frameworks like OpenSees [27], ABAQUS [32] or ANSYS [33], however it requires a lot more time and effort to develop such models in these software frameworks due to lack of user-friendly interface. Detailed FE models presented earlier also possessed the ability to simulate brittle failure mechanisms like buckling of tracks and studs. However, the detailed FE models presented here do not possess this ability because brittle failure modes were not observed in the experiment [12] of shear walls, which were designed following the capacity design approach. Though, if one wants to add such brittle failure modes capabilities to the model, it can be done by defining the limits on the stresses or strain in respective elements.

In the second approach, equivalent truss (simplified) models are developed in OpenSees for use in complete building models being analysed under the nonlinear dynamic procedures. OpenSees is a much better choice for such type of analyses, since it can perform them much faster and with less computational resources. OpenSees was also used other researchers [14–16] to develop simplified models. However, the particularity of simplified models presented here is that they can also capture brittle failure modes which could occur under in walls not designed following the capacity design approach.

Finally, using unified FE-truss models presented in the third approach, a practicing engineer can take advantage of both: the efficiency of SAP2000 in earlier phase to find the backbone, which only requires sheathing connection test results, and then the obtained backbone along with predefined cyclic parameters can be used to develop a simplified truss models in OpenSees, which directly can be used in complete building models. Even if, detailed FE model can also be developed in OpenSees but ultimately, simplified models would be needed to represent the response of shear wall in complete building models. Using SAP2000 for detailed FE models would save a lot of time and effort at least in the initial phase of unified FE-truss modelling approach.

3. Numerical modelling

3.1. Description of modelled walls

The numerical models presented in this paper were developed for CFS shear walls sheathed with nailed gypsum boards. This type of shear walls were used as the main seismic force resisting system in the double storey case study building developed within the ELISSA project [9]. The case study building was designed according to the guidelines of European construction standards [36–39], where applicable. In order to evaluate the seismic behaviour of adopted seismic force resisting system, one monotonic and three cyclic tests were conducted on different types of shear walls. In particular, three wall specimens were made of only structural elements, whereas one wall specimen was completed with all interior and exterior finishing elements. Details on the test program together with the information on geometrical, mechanical and physical properties of various elements of shear walls are provided in the companion paper [12]. The scope of this paper is only limited to the numerical modelling of shear walls without finishing elements, i.e.: WS_2400_M and WS_2400_C, which were 2.4 m long walls subjected to monotonic and cyclic loading respectively (termed as short shear walls); WS_4100_C, which was a 4.1 m long wall subjected to cyclic loading (termed as long shear wall). Table 1 provides physical and mechanical characteristics of walls and their different components, which are peculiar to the modelled shear walls.

3.2. Modelling approach

Three different types of numerical models were developed to simulate the nonlinear in-plane monotonic and cyclic response of shear walls. Initially, based on the experimental results of tests on individual sheathing connections [12], detailed FE models were developed in SAP2000 software [30] for predicting the monotonic and cyclic envelope response curves of shear walls. The main advantage of using SAP2000 is its user friendly graphical interface and its wide spread use in the civil engineering. The FE models develop is SAP2000 were also developed with an intent to serve as the guideline for the practicing engineers, who wish to simulate the response of CFS sheathed braced shear walls. In fact, SAP2000 offers various hysteretic material models (*Pivot*, *Kinematic* and *Takeda*), out of which *Pivot* model possess the least ability to simulate the pinched hysteretic response particular to sheathing connections in shear walls. Therefore, pivot model was used to simulate the cyclic response of sheathing connections. However, FE models were not able to properly predict the cyclic response of shear

Table 1
Physical and mechanical characteristics of tested shear walls.

Property	Short shear wall	Long shear wall
Wall geometry	2.4 m × 2.3 m (length × height)	4.1 m × 2.3 m (length × height)
Studs	147 × 50 × 10 × 1.5 mm (outside-to-outside web depth × flange size × lip size × thickness) mainly spaced at 625 mm on centre	
Tracks	150 × 40 × 1.5 mm (outside-to-outside web depth × flange size × thickness)	
Material for studs and tracks	S320GD + Z steel grade (characteristic yield strength: 320 MPa, characteristic ultimate tensile strength: 390 MPa)	
Sheathing panels	15.0 mm thick impact resistant special gypsum board (Knauf Diamant-X) panels on both sides of wall.	
Sheathing to steel frame connections	2.2 mm diameter ballistic nails spaced at 150 mm both at field and at the perimeter of the panels.	
Hold-downs	Simpson strong tie HTT5 devices placed at the ends of walls, connected to the wall frame via 26 self-drilling screws (5.5 mm diameter) and to the base beam by one M16 bolt (8.8 steel grade)	
Shear anchors	M8 bolts (8.8 steel grade) spaced at 300 mm	

walls as a result of convergence problems arising due to the model complexity. The pivot material model has already been used by Bourahla et al. [17] before, but in that case the complete wall response was represented by one spring element. Contrarily, in the detailed FE model presented herein, pivot model was adopted for each sheathing connection, which increased the complexity of model significantly. For this reason, the detailed FE models developed in SAP2000 software were able to predict only the monotonic response while could not predict the cyclic hysteretic response curves of shear walls.

In order to overcome the limits of detailed FE models, equivalent truss models were developed in OPENSEES software [27] using cyclic test results of shear wall [12], which could simulate the cyclic response of shear walls. Nevertheless, these equivalent truss models solely depend on the cyclic test results of shear walls for evaluating the backbone envelope and the parameters governing the cyclic behaviour. Subsequently, a unified FE-truss model was developed in OPENSEES software [27] and uses the monotonic response of shear walls obtained from FE models to define the backbone envelope of cyclic behaviour, whereas parameters governing cyclic behaviour are predefined. The only type of experimental data needed in the development of the unified FE-truss models was the test results of individual sheathing connections. Fig. 1 explains the development process of all three type of models.

In both detailed FE and equivalent truss numerical models, CFS profiles were modelled as elastic frame or truss elements, therefore they were not able to explicitly take into account the local buckling. Contrarily brittle failure modes like local buckling of CFS profiles of studs, tensile failure of anchors or tensile yielding of chord studs can be modelled by additional elements (plastic hinges, zerolength elements, ….), which can simulate these phenomena when certain threshold value of internal forces are achieved in them.

3.3. Detailed FE model

Experimental results from micro-scale tests on connections between sheathing panels and CFS frame [12] were used to predict the monotonic and cyclic envelope response of shear walls without finishing under lateral loads using a finite element model developed in SAP2000 software [30].

The shear walls were modelled as two-dimensional structures with all out-of-plane displacements restrained, i.e. displacements along Y axis and rotations about X and Z axes (Fig. 2). The CFS frame was modelled with frame elements having the actual cross section properties of profiles, with a Young's modulus of 210 GPa and a Poisson ratio equal to 0.3. Gypsum sheathing panels were modelled using linear thin shell elements having a square mesh with homogenous mechanical properties throughout its surface area. Mesh size of 50 × 50 mm and a thickness of 15 mm was used for thin shell elements. A shear modulus of elasticity equal to 2400 MPa and a Poisson ratio equal to 0.3 was used to represent the material properties of the sheathing panels. These shell elements were modelled on both sides of CFS frame. Hold-downs present at both bottom ends of walls were modelled using a simple support, which restrain horizontal displacements, and a vertical linear springs having a stiffness of 37 kN/mm, which was obtained based on displacements measured at hold down devices during the experiments [12]. The shear anchors placed on the bottom wall track were schematized as pinned restraints. Connections between studs and tracks were modelled as hinge connections. Rigid diaphragm effect was incorporated by applying a body constraint to the top track.

Connections between sheathing panels and CFS frame were modelled using the nonlinear link element with a multi-linear backbone curve, which represents the main nonlinear source in the walls. The link force (F) - displacement (δ) relationships were defined only for translational displacements along X and Z axes. Results of monotonic and cyclic tests on the sheathing connections were used to define the backbone curves of nonlinear links. For a given model, same backbone curve was defined for both X and Z degree of freedoms. This assumption is a simplified way to account for the resulting behaviour of sheathing connection in terms of shear response in X and Z directions. The real path of the fasteners, as well as the local deformation due to the tilting and pull-out of nails observed during the experiments was not explicitly modelled. Though, the most realistic way to model sheathing connections would be to use an element which takes in to account the real path of the deformation, e.g. the radial spring element as defined in Ding [24] However, the use of two perpendicular link elements in this study also showed good performance as it shown in the results discussed later on. In particular, three different multi-linear backbone curves were used to model the walls WS_2400_M, WS_2400_C and WS_4100_C. For short shear walls subjected to monotonic (WS_2400_M) and cyclic (WS_2400_C) loading, multi-linear backbone curves were assigned on the basis of monotonic and cyclic connection tests results [12], as shown in Fig. 3a and b, respectively. For the model of the long shear

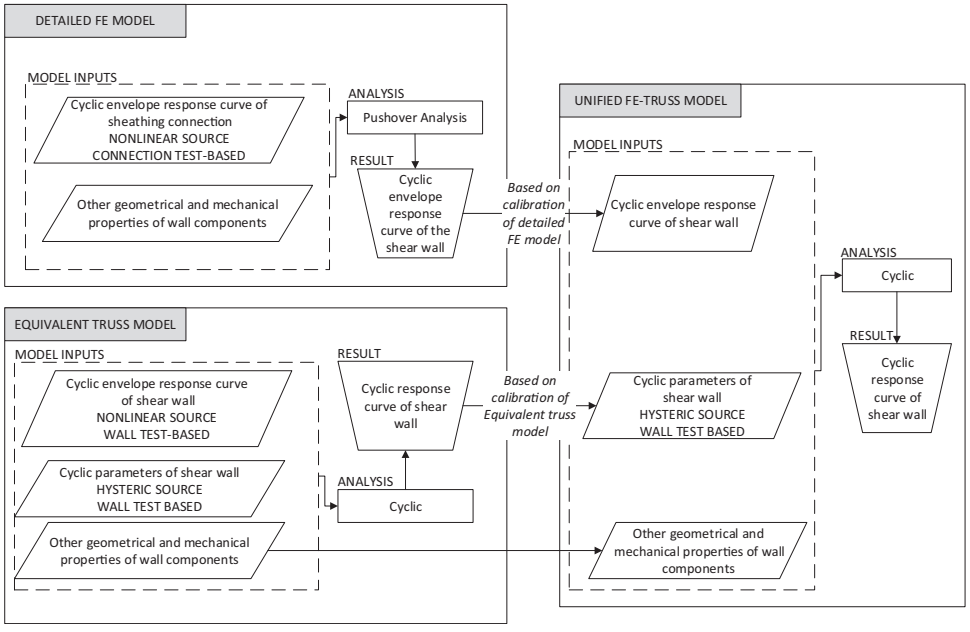

Fig. 1. Modelling approach for models presented in the paper.

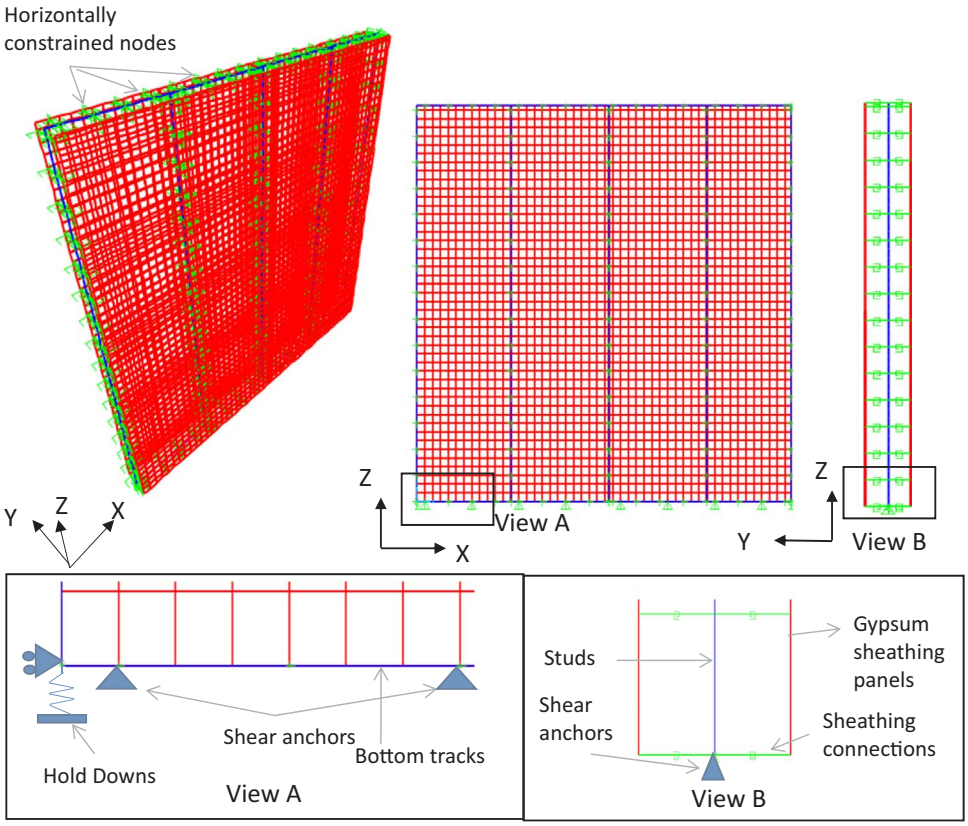

Fig. 2. Schematization of detailed finite element model developed for CFS sheathed braced shear walls.

wall (WS_4100_C), two types of multi-linear backbone curves were used for the sheathing connections. Connection between panel edges and internal studs were modelled as imperfect connection on the bases of test results obtained for specimens representative of defects in assembling (termed as "uncontrolled" specimens in companion paper [12]). In particular, "uncontrolled" connections resulted in a peak strength reduced of 40% in comparison with that of properly assembled connection. Fig. 4 compares the average backbone envelope curves of cyclic test results on perfect and imperfect connections, whereas Fig. 5 illustrates the location of imperfect connections in the long shear wall. All other sheathing connections were modelled as perfect connections, for whom the backbone curve is obtained on the basis of cyclic tests as shown in Fig. 3b.

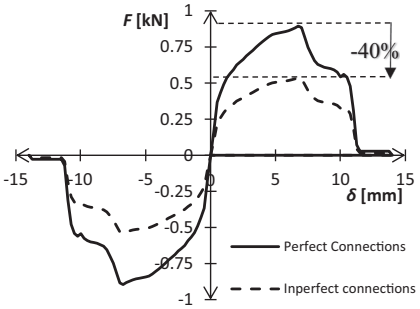

Fig. 4. Comparison of average backbone envelope curves of cyclic tests on perfect and imperfect connections.

3.4. Detailed FE model vs experimental results

Results of pushover analyses were compared against the monotonic and cyclic test results [12]. Numerical models were able to simulate with good accuracy the deformation mechanism observed during the tests, which was characterized by a typical behaviour of sheathed CFS shear walls designed according to capacity design rules (Fig. 6), in which the CFS frame deforms into a parallelogram and sheathing panels rotate in their plane, leading to the most ductile failure mechanism, i.e.

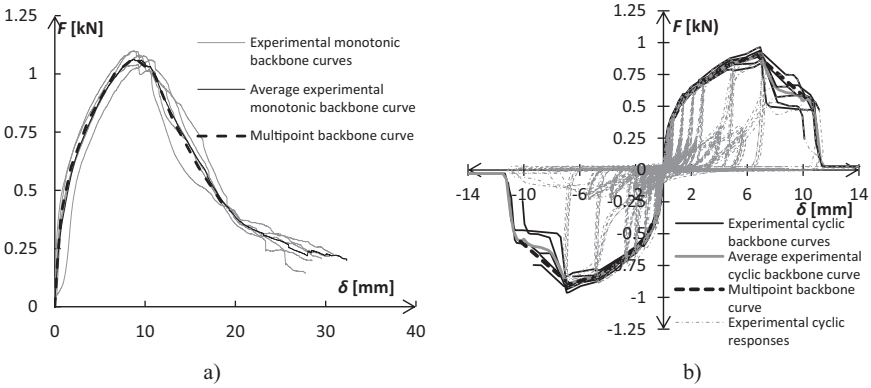

Fig. 3. Backbone envelope used for nonlinear links based on experimental a) monotonic and b) cyclic response of connections.

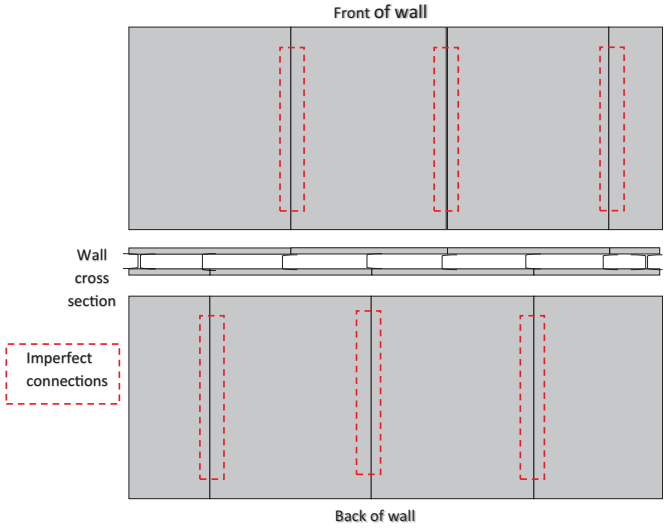

Fig. 5. Location of imperfect connections on long shear wall.

sheathing connection failure. The comparison between experimental and numerical results in terms of lateral force (H) vs top displacement (d) curve is shown in Fig. 7 for all shear walls.

All models provided good results until reaching the maximum strength, whereas the post-peak behaviour in case of cyclically tested walls was underestimated by FE models. The main reason behind the underestimation of post-peak response is the post-peak shape of sheathing connections backbone envelope, which is characterized by a higher slope respect to those showed by walls. Performance of FE models was quantitatively evaluated by considering three parameters: conventional elastic stiffness (k_e), peak strength (H_p) and conventional ultimate displacement (d_u). In particular, the peak strength (H_p) is the maximum recorded load, the conventional elastic stiffness (k_e) represents the secant stiffness evaluated to the 40% of the peak shear strength (H_p), and the ultimate displacement (d_u) is the displacement corresponding to the 80% of the peak shear strength evaluated on the post-peak branch of force (H) – displacement (d) curve. From examination of results (Fig. 7) it can be observed that FE models capture very well the wall resistance, with a slight overestimation of the peak strength (from 3% to 7%). On contrary, as observed above about the comparison in terms of post-peak behaviour, the numerical response underestimates the ultimate displacement (from 5% to 35%). Finally, the prevision of the elastic stiffness is underestimated (of 15%) for the monotonic test and overestimated for the cyclic tests (from 27% to 31%). These results confirm the well-known major difficulty of numerical models for the evaluation of deflections with respect to strengths. A similar range of error tolerances (−17% to 38%) were also reported by Buonopane et al. [20] for the detailed FE model developed in OpenSees. In addition, due to the high nonlinear lateral response (without an initial linear behaviour) of these structural systems, the comparison in terms of elastic stiffness is not simple. For this reason, the comparison has to be performed in a conventional way, and it has secondary relevance with respect to structural systems characterized by a clear initial linear lateral response. However, considering the whole response curves, the numerical previsions are overall on the safe side (underestimation of the dissipated energy, i.e. the area under the $H - d$ curve).

3.5. Equivalent truss model

The simulation of nonlinear dynamic behaviour of shear walls is crucial to the collapse simulation of whole building models for achieving the objectives of PBSD. The detailed FE models presented earlier were able to predict the nonlinear pushover response of shear walls with good accuracy, but they lacked the ability to simulate the wall cyclic response. This limitation is mainly due to the inherent complexity of these models, which considerably increases the time of analysis and computing resources. In this regard, an equivalent truss model was developed for both short (WS_2400_C) and long (WS_4100_C) shear walls, which could simulate the deteriorating hysteretic behaviour of shear walls and easily be used for whole building modelling.

OpenSees software [27] was used for this purpose. In particular, walls were schematized through two-dimensional models (Fig. 8) having three degrees of freedom, i.e. vertical and horizontal translation and in plane rotation. The nonlinear behaviour of walls was represented by a pair of nonlinear *truss elements* placed in a X configuration and connected to the pinned frame. The vertical frame elements representing the chord studs were modelled using *truss elements* with a *Uniaxial elastic material*, having modulus of elasticity of 210 GPa. The *Opensees MinMax material* was used in conjunction with *uniaxial elastic material* in order to simulate the chord stud failure due to tension or global buckling. *Opensees MinMax material* is always used in conjunction with another material, which define its stress-strain behaviour, and it enforces the threshold values of strain, beyond which strength and stiffness of element are set to zero. In the specific case, threshold values, which govern the occurrence of failure of studs in tension ($\varepsilon_{t,Rk}$) and compression ($\varepsilon_{b,Rk}$), were calculated using Eqs. (1) and (2).

$$\varepsilon_{t,Rk} = \frac{N_{t,Rk}}{A \cdot E} \tag{1}$$

$$\varepsilon_{b,Rk} = \frac{N_{b,Rk}}{A \cdot E} \tag{2}$$

where: $N_{t,Rk}$ = 247 kN and $N_{b,Rk}$ = 123 kN are, the nominal resistances corresponding to the tensile and buckling failure of chord studs, respectively; E is the Young's modulus of steel; A is gross cross section area. $N_{t,Rk}$ and $N_{b,Rk}$ are obtained according to prescriptions given in EN

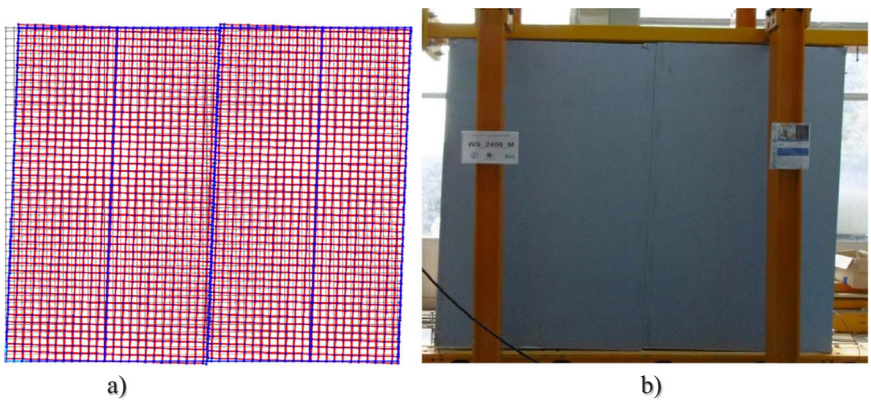

Fig. 6. Deformed shape of short shear wall (WS_2400_M) a) finite element model b) monotonic tests.

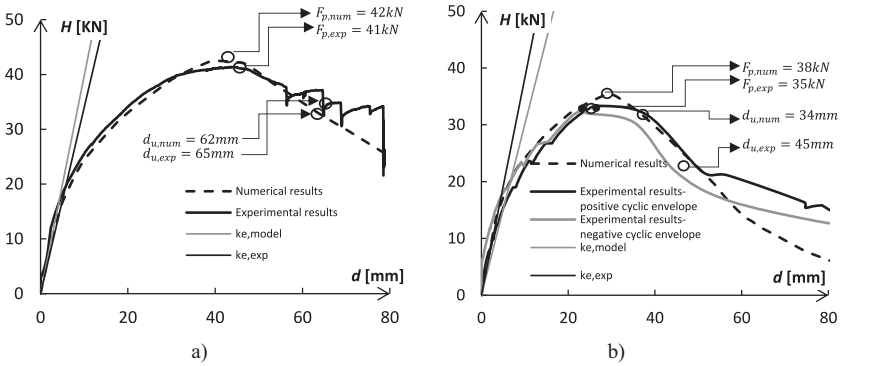

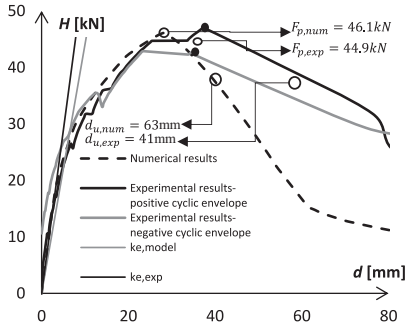

Wall label	WS_2400_M	WS_2400_C	WS_4100_C	Average
$K_e \frac{Num}{Exp}$	0.85	1.27	1.31	1.14
$H_p \frac{Num}{Exp}$	1.03	1.07	1.03	1.04
$d_u \frac{Num}{Exp}$	0.95	0.75	0.65	0.78

d)

Fig. 7. Comparison of the short wall numerical models a) (WS_2400_M) with its monotonic test response b) (WS_2400_C) with its cyclic test response c) (WS_4100_C) with its cyclic test response d) quantitative comparison of numerical and experimental results.

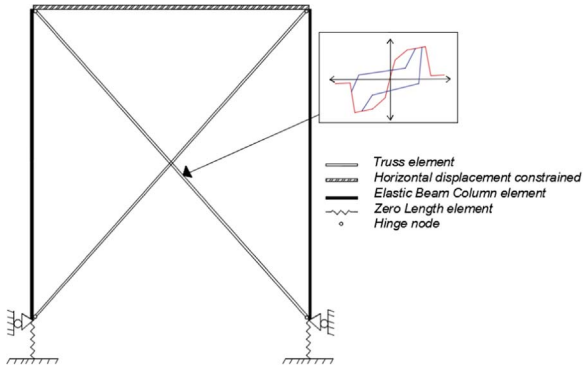

Fig. 8. Schematization of simplified truss model developed for CFS sheathed-braced shear walls.

1993-1-1 [37] and EN 1993-1-3 [38]. Stiffness contribution through hold-down anchors to foundation was modelled by using *Zerolength elements* of unit area placed at the bottom of the ends studs. *ElasticMultiLinear material* with a stiffness k_a = 37 kN/mm in tension and a very high stiffness (10,000 kN/mm) in compression was used for *Zerolength elements*. In OpenSees [27] definition of *ElasticMultiLinear material* the stress-strain relationship is given by a multi-linear curve that is defined by a set of points. The loading and unloading occur along the multi-linear curve in a nonlinear way without any energy dissipation. *MinMax material* was used in conjunction with *ElasticMultiLinear material* in order to take into account tensile failure of anchors. For this purpose, tensile strain in *MinMax material* was set to not exceed the nominal tensile strain $\varepsilon_{a,Rk}$ of anchors, whereas there was no strain limit in compression. In particular, nominal tensile strain in anchors $\varepsilon_{a,Rk}$ is calculated using Eq. (3):

$$\varepsilon_{a,Rk} l_a = \frac{N_{a,Rk}}{k_a} \tag{3}$$

where $N_{a,Rk}$ = 43 kN is the nominal tensile resistance of anchors and l_a represents unit length of an anchor. Rigid diaphragm effect was incorporated by constraining the horizontal displacements at the wall top, using *EqualDOF* command. *P-Δ* effects were neglected because there were no gravity loads present in the tests [12].

Pinchinng4 material [28] was used to represent the nonlinearity in truss elements. Choice of *Pinchinng4 material* was motivated by the appreciable results obtained by other researchers who used it to simulate response of CFS shear walls [14,20,40]. *Pinching4 material* is a uniaxial material that can represent pinched load deformation response with the ability to exhibit degradation under cyclic loading. In particular, the material rule can be defined through the set of 39 parameters. It includes 16 parameters for the definition of the backbone curve (*ePf1, ePd1, ePf2, ePd2, ePf3, ePd3, ePf4, ePd4, eNf1, eNd1, eNf2, eNd2, eNf3, eNd3, eNf4, eNd4*), 6 parameters for defining the cyclic behaviour (*uForceP, uForceN, rDispP, rDispN, rForceP, rForceN*), 5 parameters for governing the strength degradation (*gF1, gF2, gF3, gF4, gFLim*), 5 parameters for controlling the unloading stiffness degradation (*gK1, gK2, gK3, gK4, gKLim*), 5 parameters for controlling the reloading stiffness degradation (*gD1, gD2, gD3, gD4, gDLim*), and 2 parameters for limiting the maximum degradation in each cycle (*gE, dmgType*). The key parameters used in the study to define *Pinching4 material* are illustrated in Fig. 9. These parameters were selected based on the cyclic test results on shear walls [12]. The calibration of *Pinchinng4 material* was carried out through a two-step process: initially the parameters representing the backbone curve were selected to capture the complete hysteretic envelope and later on the cyclic and degradation parameter were adjusted to achieve a good match between the hysteretic response

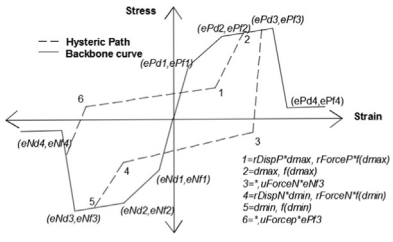

Fig. 9. OpenSees definition of Pinching4 material.

obtained from the models and experimental results.

In Fig. 9 points (*ePd1, ePf1*) to (*ePd4, ePf4*) and (*eNd1, eNf1*) to (*eNd4, eNf4*) represent the positive and negative branch of the backbone envelope curve in terms of stress and strain, respectively. This 4-points backbone curve was adjusted to capture entire envelope of hysteretic behaviour. In particular, the 4-points were defined considering the average envelope curve obtained considering positive and negative branches. Therefore, symmetric values of these parameters were used for both positive and negative branches and only 8 independent parameters were defined (*ePdi = eNdi, ePfi = eNfi*). Eqs. (4)–(6) were used to transform force and displacement from experimental results into stress and strain of *Pinching4 material* used in the numerical model.

$$f = \frac{H}{2\cdot\cos(\theta)} \tag{4}$$

$$d_\theta = d\cos(\theta) \tag{5}$$

$$strain = \frac{d_\theta}{l} = \frac{d\cos(\theta)}{l} \tag{6}$$

where: H is the force applied during the test; d is the top wall displacement recorded during the test; f is the stress in a strap of unit area; d_θ is the axial deformation in the strap; l is the length of the strap; and θ is the angle of the diagonal strap respect to bottom track.

First point of the numerical backbone curve (start point, S) was positioned on the experimental envelope curve at the 20% of the peak strength (H_P), in such a way to allow the models to capture nonlinear behaviour of walls from start and to dissipate energy in the initial cycles. The force at second point of the numerical backbone curve (intermediate point, I) was set equal to 80% of H_p, whereas the displacement was chosen with an energy balance, so that the area under the numerical backbone curve until peak is equal to that of the experimental envelope curve. Third point of the numerical backbone curve (peak point, P) was set equal to the peak point of the experimental envelope curve. The displacement at fourth point of numerical backbone curve (ultimate point, U) was set equal to 2.5%, whereas the force was selected with an energy balance, so that the area under the numerical backbone curve between third and fourth point is equal to that of the experimental envelope curve. Fig. 10 shows the comparison of numerical backbone curves used in equivalent truss model of short and long shear walls with the relevant experimental envelope curves.

Unloading and reloading paths are controlled by series of force and displacement ratios, which include positive (*uForceP*, *rDispP* and *rForceP*) and negative (*uForceN*, *rDispN* and *rForceN*) parameters. As regards to positive branches, *uForceP* defines the ratio between the strength developed upon unloading and maximum strength of the positive backbone curve. *rDispP* and *rForceP* mark the strength and displacement at which reloading occurs. In particular, *rForceP* is the ratio between the strength of reloading point and strength at maximum positive displacement of preceding cycles. *rDispP* is the ratio between the displacement of the reloading point and maximum positive displacement of preceding cycles. Obviously, same definitions apply for negative branches (*uForceN, rDispN, rForceN*). Symmetric values of these parameters were used for both positive and negative branches of hysteretic path. Therefore, only 3 independent parameters were defined (*uForceP = uForceN*, *rDispP = rDispN* and *rForceP = rForceN*). In particular, *uForce, rDisp* and *rForce* were selected and calibrated in a way to achieve good match with respect to experimental results, in terms of force vs. displacement relationship and dissipated energy. Since in experimental results unloading branch nearly approaches zero for all cycles, therefore *uForce* was taken equal to 0. The reloading points on experimental curves were characterized by very low values of force, therefore *rForce* was set equal to 0.1. *rDisp* was calibrated by varying the values in the range from 0.1 to 1.0 and selecting the value that minimizes, for each shear wall model, the square error in terms of dissipated energy. The obtained values for *rDisp* were 0.45 and 0.50 for short and long shear walls, respectively. The rest of the 17 parameters governing strength and stiffness degradation were also calibrated in a way to achieve the good match with experimental results. Table 2 summarizes the properties of *Pinching4 material* used for both short and long shear wall models.

Table 2
Properties of Pinching4 material used for short and long shear wall models.

Model	Short wall (WS2400M_C)	Long wall (WS4100M_C)
Parameters for backbone curve		
ePf1 (kN)	4.8	5.1
ePf2 (kN)	19.1	20.6
ePf3 (kN)	23.8	25.7
ePf4 (kN)	9.8	17.4
ePd1	0.0002	0.0001
ePd2	0.0024	0.0015
ePd3	0.0050	0.0067
ePd4	0.0161	0.0141
Parameters for cyclic behaviour		
uForce	0	0
rDisp	0.45	0.50
rForce	0.1	0.1
gF,1,2	0	0
gF,3,4	0	0
gF,Lim	0	0
gK,1,2	1.2	1.2
gK,3,4	1.2	1.2
gK,Lim	0.9	0.9
gD,1,2	0.2	0.2
gD,3,4	1.2	1.2
gD,Lim	0.4	0.4
gE	10	10
dmgType	energy	energy

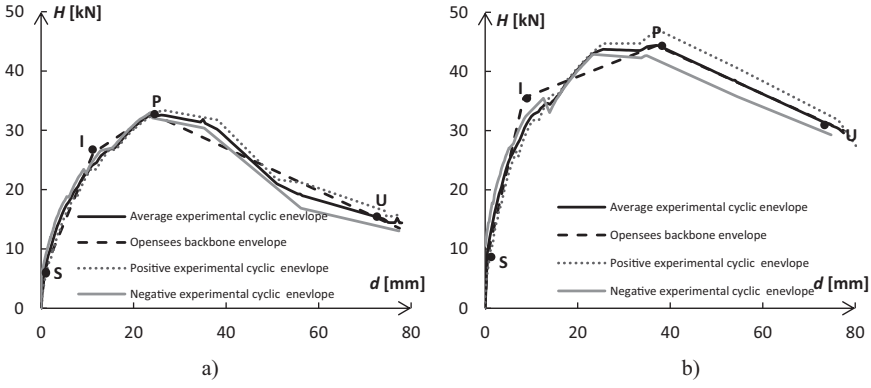

Fig. 10. Comparison between numerical backbone and experimental envelope curves for short (a) and long (b) walls.

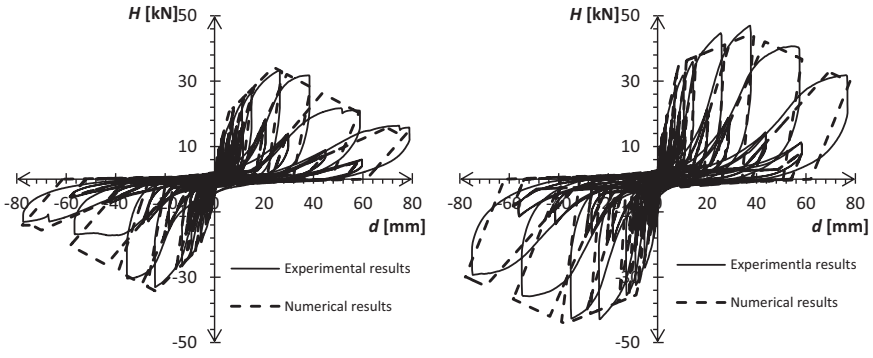

Fig. 11. Comparison of force vs displacement response between numerical model and cyclic test for a) short shear wall (WS_2400_C) a) b long shear wall (WS_4100_C).

3.6. Equivalent truss model vs experimental results

The Equivalent truss model was used to simulate the quasi-static cyclic tests conducted on short and long shear walls. For this purpose, the same cyclic loading protocol used in the reference tests was imposed at the top of shear walls. In particular, the loading protocol used for the experimental activity is the CUREE ordinary ground motions reversed cyclic load developed by Krawinkler et al. [41] for wood shear walls. The loading protocol consists of initiation, primary and trailing cycles. More details on the loading protocol can be found in the companion paper [12]. Fig. 11 illustrates force vs displacement response curves of both numerical models and cyclic test results obtained for short (WS_2400_C) and long (WS_4100_C) shear walls.

It can be noticed that numerical models were able to capture the experimental hysteretic response in terms of overall shape and location of peaks. Quantitative comparison of the energy dissipated by numerical and experimental results was made using Eqs. (7)–(10).

$$CE_{e,j} = \sum_{i=1}^{j} E_{e,i}, [i, j \le n] \tag{7}$$

$$CE_{n,j} = \sum_{i=1}^{j} E_{n,i}, [i, j \le n] \tag{8}$$

$$\Delta_{E,i} = \frac{E_{n,i} - E_{e,i}}{E_{e,i}} \times 100, \ [i \le n] \tag{9}$$

$$\Delta_{CE,j} = \frac{CE_{n,j} - CE_{e,j}}{CE_{e,j}} \times 100, \ [j \le n] \tag{10}$$

where: $CE_{e,j}$ and $CE_{n,j}$ represent the cumulative energy dissipated for jth cycle of the loading protocol obtained in experimental and numerical results, respectively; $E_{e,i}$ and $E_{n,i}$ represent the energy dissipated in ith cycle of experimental and numerical results, respectively; $\Delta_{E,i}$ is the percentage difference of the energy dissipation for ith cycle of loading protocol between numerical and experimental results; $\Delta_{CE,j}$ is the percentage difference of the cumulative energy for the jth cycle of loading protocol between numerical and experimental results; n is the last cycle of the loading protocol. Fig. 12 show the comparison in terms of cumulative energy dissipation between the numerical and experimental results for the short and long shear walls.

Numerical models were able to dissipate energy in a similar manner to the experimental tests. In the case of the short wall, the numerical model underestimated the cumulative energy for the first 32 cycles of the loading protocol, whereas it slightly overestimated the cumulative energy in subsequent cycles. Similarly, for the long wall the prevision of the numerical model gave an underestimation of the cumulative energy in the first 28 cycles, whereas it slightly overestimated the cumulative energy in the rest of cycles. For primary cycles, the average of the absolute values of the error $\Delta_{E,i}$ was 22% and 11% for short and long shear walls, respectively. The absolute difference in cumulative energy $\Delta_{CE,j}$ dissipated by all primary cycles was 3% and 2% for short and long shear walls, respectively; whereas the cumulative error $\Delta_{CE,n}$ at the 43rd cycle of loading protocol was 4% and 5% for short and long walls, respectively.

3.7. Unified FE-truss models

This section presents an approach to develop a numerical model which only uses the experimental results of sheathing connection tests to simulate the nonlinear cyclic response of sheathed CFS shear walls. The presented modelling approach is then validated through the simulation of nonlinear cyclic response of short (WS_2400_C) and long (WS_4100_C) walls.

The equivalent truss model presented earlier used *Pinching4 material* [28] calibrated on the basis of experimental results to simulate the nonlinear hysteretic response of shear walls in OpenSees software [27]. In particular, both backbone envelope and cyclic parameters of *Pinching4 material* had been derived on the basis of experimental cyclic test results. On contrary, the model presented herein uses the backbone curve of *Pinching4 material* derived from the detailed FE model developed in Section 3.3, which use only connection test results as input, whereas the cyclic parameters are assumed on the basis of calibration

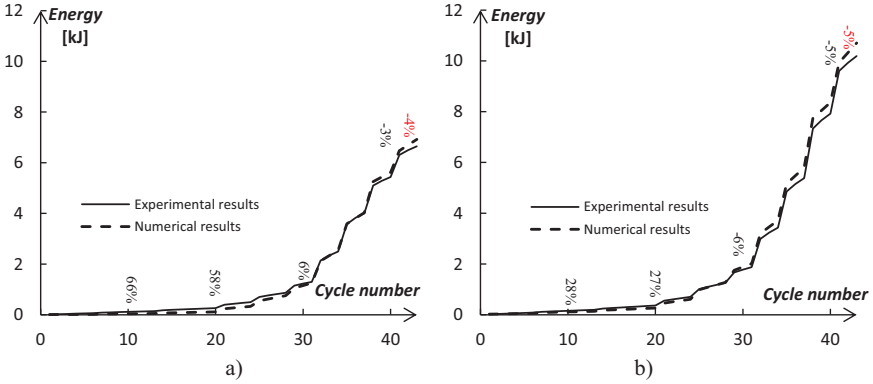

Fig. 12. Comparison of energy dissipation between numerical model and cyclic test for a) short shear wall (WS_2400_C) and b) long shear wall (WS_4100_C).

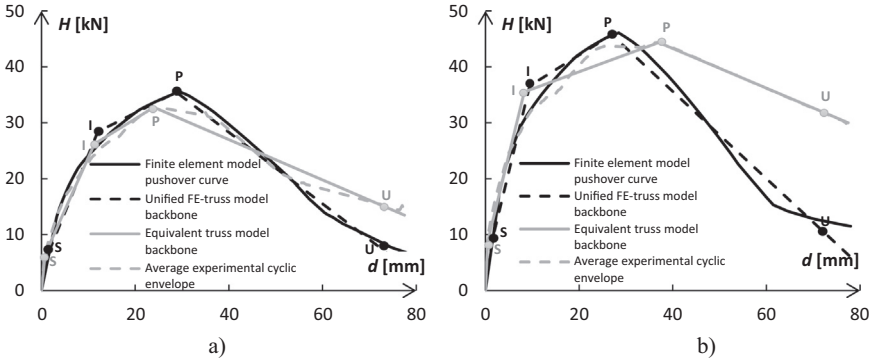

Fig. 13. Comparison between numerical backbone curves used in the unified-truss model and equivalent truss model for short (a) and long (b) walls.

results of equivalent truss model (Section 3.5). In fact, the only difference in the cyclic parameters for short and long walls in Section 3.5 was *rDisp*. In particular, *rDisp* was 0.45 and 0.50 for short and long walls, respectively (Table 2). The model presented here in uses an average value of 0.475 for *rDisp*. Following this approach, the need of cyclic test results of shear walls for calibration can be overcomed.

The procedure for defining the backbone curve is the same as that used in Section 3.5, i.e. the definition of points S, I, P and U starting from the pushover curve obtained from detailed FE models. Fig. 13 shows the comparison between numerical backbone curves used in the Unified-truss model and Equivalent truss model for both short and long walls. Obviously, since the Detailed FE models underestimated the post-peak responses, therefore the slopes of post-peak branches of backbone curves adopted in Unified-truss models were higher than those of Equivalent truss models, especially in the case of the long wall.

3.8. Unified FE-truss model vs experimental results

In order to evaluate the accuracy of the approach presented above, numerical models of both short (WS_2400_C) and long (WS_4100_C) walls are developed and their performance is compared with the relevant experimental results [12]. Obviously, the same cyclic loading protocol is used for this purpose. From Fig. 14, it can be noticed that numerical models are able to represent the cyclic behaviour of walls with quite good accuracy in terms of overall shape of force-displacement response curves. In particular, the provision of the Unified FE-truss model was worse for cycles having amplitudes higher than displacements corresponding to peak strengths, especially in the case of the long wall. Obviously, this was due to the shape of the adopted backbone curves, as discussed earlier. Fig. 15 shows the comparison between the numerical and experimental results in terms of cumulative cycle energy dissipation for the short and long walls.

Numerical models underestimated the cumulative energy in comparison with the experimental results for all cycles of loading protocol for both short and long walls. In particular, for primary cycles the average of the absolute values of the error $\Delta_{E,i}$ was 35% and 47% for short and long walls, respectively. The absolute difference in cumulative energy $\Delta_{CE,j}$ dissipated in all primary cycles was 18% and 35% for short and long, respectively; whereas the cumulative error $\Delta_{CE,n}$ at the 43rd cycle of loading protocol was 24% and 40% for short and long walls, respectively.

4. Conclusions

This paper presents the three-different type of numerical models developed for CFS gypsum sheathed braced shear walls that were tested monotonically and cyclically under the framework of project ELISSA. The first type of model is a Detailed FE model, which requires experimental results of sheathing connection tests as main input. The model is able to predict the in-plane nonlinear pushover response of shear walls with very good accuracy up to the peak strength, whereas it underestimates the post-peak response. One of the benefits of this FE model is the very less amount of experimental evidence required for its development, which can be carried out with ease in modern day to day commercial structural analysis software's like SAP2000. FE models developed in this study could prove useful for a practicing engineer to estimate strength and stiffness of single shear wall, while only using the sheathing connection test results. The second type of model was more simplified and used a pair of nonlinear truss elements to represent the cyclic nonlinear response of walls. This Equivalent truss model was able to simulate the nonlinear cyclic response of shear walls with good accuracy, but requires experimental results of shear wall tests as main input. The simplicity of this model allows them to be used into whole building models, which can be analysed under the action of selected ground motions to meet the PBSD objectives. In the end, a third type of model (Unified FE-truss model) is presented to simulate the nonlinear cyclic response of shear walls, which rely only on the sheathing connection test results and subsequently eliminates the need of cyclic tests

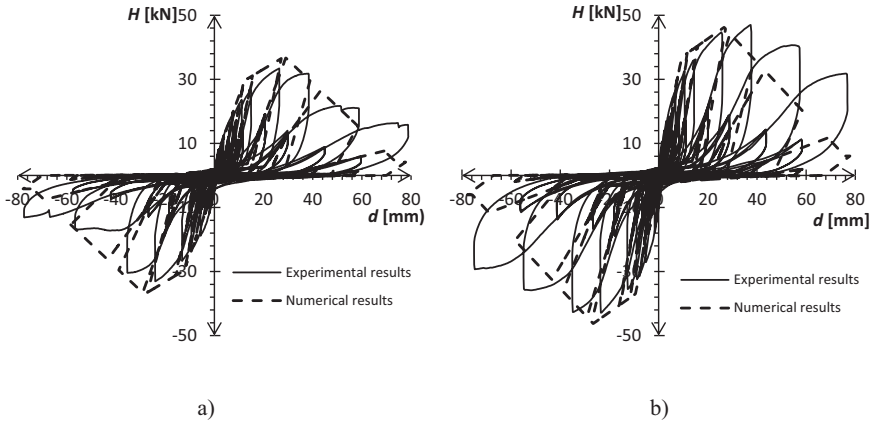

Fig. 14. Comparison of force vs displacement response between unified numerical model and cyclic test for a) short shear wall (WS_2400_C) and b) long shear wall (WS_4100_C).

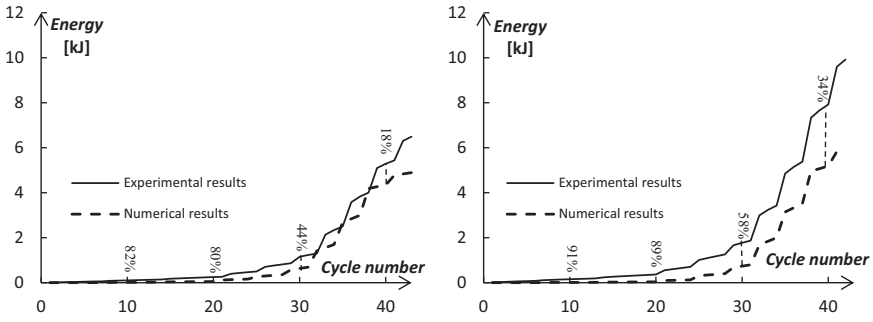

Fig. 15. Comparison of energy dissipation between unified numerical model and cyclic test for a) short shear wall (WS_2400_C) and b) long shear wall (WS_4100_C).

on complete shear walls for calibration. The performance comparison of Unified FE-truss model against the test results of shear walls revealed its ability to simulate the nonlinear hysteretic response of shear walls with acceptable accuracy and results on the safe side, i.e. underestimation of the dissipated energy of numerical simulations in comparison with experimental results. The cyclic parameters used in unified-FE models are obtained from truss models which are calibrated on the basis of mere three experiments. Certainly, it requires a much wider experimental database for the calibration of cyclic parameters, which could be the focus of future studies.

Acknowledgements

The study presented in this paper is a part of the project "Energy Efficient LIghtweight-Sustainable-SAfe-Steel Construction" (Project acronym: ELISSA) coordinated by Prof. Raffaele Landolfo for the activities of the University at Naples “Federico II”. The project has received funding from the European Union Seventh Framework Programme (FP7/2007-2013) under grant agreement no. 609086. The authors would also like to thank the ELISSA consortium for the collaboration.

References

[1] L. Fiorino, O. Iuorio, R. Landolfo, Sheathed cold-formed steel housing: a seismic design procedure, Thin-Walled Struct. 47 (2009) 919–930, http://dx.doi.org/10.1016/j.tws.2009.02.004.
[2] L. Fiorino, O. Iuorio, R. Landolfo, Seismic analysis of sheathing-braced cold-formed steel structures, Eng. Struct. 34 (2011) 538–547, http://dx.doi.org/10.1016/j.engstruct.2011.09.002.
[3] L. Fiorino, O. Iuorio, V. MacIllo, R. Landolfo, Performance-based design of sheathed CFS buildings in seismic area, Thin-Walled Struct. 61 (2012) 248–257, http://dx.doi.org/10.1016/j.tws.2012.03.022.
[4] L. Fiorino, G. Della Corte, R. Landolfo, Experimental tests on typical screw connections for cold-formed steel housing, Eng. Struct. 29 (2007) 1761–1773, http://dx.doi.org/10.1016/j.engstruct.2006.09.006.
[5] R. Landolfo, Cold-formed steel structures in seismic area : research and applications, in: Proceedings of the VIII Congresso de Construção Metálica e Mista, Guimarães, Portugal, 2011, pp. 3–22.
[6] O. Iuorio, L. Fiorino, R. Landolfo, Testing CFS structures: the new school BFS in Naples, Thin-Walled Struct. 84 (2014) 275–288, http://dx.doi.org/10.1016/j.tws.2014.06.006.
[7] L. Fiorino, O. Iuorio, R. Landolfo, Designing CFS structures: the new school bfs in naples, Thin-Walled Struct. 78 (2014) 37–47, http://dx.doi.org/10.1016/j.tws.2013.12.008.
[8] L. Fiorino, V. Macillo, M.T. Terracciano, T. Pali, B. Bucciero, R. Landolfo, Experimental tests for the seismic response evaluation of cold-formed steel shear walls sheathed with nailed gypsum- based panels, in: Proceedings of the International Specialty Conference on Cold-Formed Steel Structures, Baltimore, USA, 2016, p. 6.
[9] L. Fiorino, V. Macillo, R. Landolfo, Shake table tests of a full-scale two-story sheathing-braced cold-formed steel building, Eng. Struct. 151 (2017) 633–647, http://dx.doi.org/10.1016/j.engstruct.2017.08.056.
[10] L. Fiorino, V. Macillo, R. Landolfo, Experimental characterization of quick mechanical connecting systems for cold-formed steel structures (136943321667131), Adv. Struct. Eng. (2016), http://dx.doi.org/10.1177/1369433216671318.
[11] G.C. Foliente, Developments in performance-based building codes and standards, For. Prod. J. 50 (2000).
[12] V. Macillo, L. Fiorino, R. Landolfo, Seismic response of cold-formed steel shear walls sheathed with nailed gypsum panels: experimental tests, Thin-Walled Struct. 120 (2017) 161–171, http://dx.doi.org/10.1016/j.tws.2017.08.022.
[13] L. Fülöp, D. Dubina, Performance of wall-stud cold-formed shear panels under monotonic and cyclic loading: part II: numerical modelling and performance analysis, Thin-Walled Struct. 42 (2004) 339–349, http://dx.doi.org/10.1016/S0263-8231(03)00064-8.
[14] I. Shamim, C.a. Rogers, Steel sheathed/CFS framed shear walls under dynamic loading: numerical modelling and calibration, Thin-Walled Struct. 71 (2013) 57–71, http://dx.doi.org/10.1016/j.tws.2013.05.007.
[15] J. Leng, B.W. Schafer, S.G. Buonopane, Seismic computational analysis of CFS-NEES building, in: Proceedings of the International Specialty Conference on Cold-Formed Steel Structures, 2012, p. 4.
[16] S. Kechidi, N. Bourahla, Deteriorating hysteresis model for cold-formed steel shear wall panel based on its physical and mechanical characteristics, Thin-Walled Struct. 98 (2016) 421–430, http://dx.doi.org/10.1016/j.tws.2015.09.022.
[17] N. Bourahla, T. Boukhemacha, N. Allal, A. Attar, Equivalent shear link modeling and performance analysis of cold formed steel structures under earthquake loading, in: Proceedings of the 9th U.S. National and 10th Canadian Conference on Earthquake Engineering, 2010.
[18] M. Nithyadharan, V. Kalyanaraman, Modelling hysteretic behaviour of cold-formed steel wall panels, Eng. Struct. 46 (2013) 643–652, http://dx.doi.org/10.1016/j.engstruct.2012.08.022.
[19] J. Martínez-Martínez, L. Xu, Simplified nonlinear finite element analysis of buildings with CFS shear wall panels, J. Constr. Steel Res. 67 (2011) 565–575, http://dx.doi.org/10.1016/j.jcsr.2010.12.005.
[20] S.G. Buonopane, G. Bian, T.H. Tun, B.W. Schafer, Computationally efficient fastener-based models of cold-formed steel shear walls with wood sheathing, J. Constr. Steel Res. 110 (2015) 137–148, http://dx.doi.org/10.1016/j.jcsr.2015.03.008.
[21] S. Esmaeili Niari, B. Rafezy, K. Abedi, Seismic behavior of steel sheathed cold-formed steel shear wall: experimental investigation and numerical modeling, Thin-Walled Struct. 96 (2015) 337–347, http://dx.doi.org/10.1016/j.tws.2015.08.024.
[22] X. Zhou, Y. He, Y. Shi, T. Zhou, Y. Liu, Experiment and FE Analysis on Shear Resistance of Cold-Formed Steel Stud Assembled Wall in Residential Structure, 2010. ⟨https://dx.doi.org/10.18057/IJASC.2010.6.3.7⟩.
[23] Y. Telue, M. Mahendran, Behaviour and design of cold-formed steel wall frames lined with plasterboard on both sides, Eng. Struct. 26 (2004) 567–579, http://dx.doi.org/10.1016/j.engstruct.2003.12.003.
[24] C. Ding, Monotonic and Cyclic Simulation of Screw-Fastened Connections for Cold-Formed Steel Framing, Virginia Polytechnic Institute and State University, Blacksburg, VA, 2015https://vtechworks.lib.vt.edu/handle/10919/55270.
[25] V. Parkash, G.H. Powell, S. Campbell, Drain-3DX Base Program Description and User Guide, 1994.
[26] L. Fülöp, D. Dubina, Performance of wall-stud cold-formed shear panels under monotonic and cyclic loading part I: experimental research, Thin-Walled Struct. 42 (2004) 321–338, http://dx.doi.org/10.1016/S0263-8231(03)00063-6.
[27] S. Mazzoni, F. McKenna, M.H. Scott, G.L. Fenves, Open System for Earthquake Engineering (OpenSees), 2009.
[28] L.N. Lowes, N. Mitra, A. Altoontash, A Beam-Column Joint Model for Simulating the Earthquake Response of Reinforced Concrete Frames, Berkeley, 2004.
[29] B.W. Schafer, D. Ayhan, J. Leng, P. Liu, D. Padilla-Llano, K.D. Peterman, et al., Seismic response and engineering of cold-formed steel framed buildings, Structures 8 (2016) 197–212, http://dx.doi.org/10.1016/j.istruc.2016.05.009.
[30] CSI, Structural Analysis Program SAP2000, 2016. ⟨https://www.csiamerica.com/products/sap2000⟩.
[31] G.C. Foliente, Hysteresis modeling of wood joints and structural systems, J. Struct. Eng. 121 (1995) 1013–1022, http://dx.doi.org/10.1061/(ASCE)0733-9445(1995)121:6(1013).
[32] HKS, ABAQUS/Standard Users Manual, 1996. ⟨https://www.3ds.com/products-services/simulia/products/abaqus/⟩.
[33] Swanson Analysis Systems Inc. (SASI), ANSYS, 1994.
[34] S. Kechidi, N. Bourahla, J. Miguel, Seismic Design Procedure for Cold-Formed Steel Sheathed Shear Wall Frames: Proposal and Evaluation, 128, 2017, pp. 219–232.
[35] I. Shamim, C.A. Rogers, Numerical evaluation: AISI S400 steel-sheathed CFS framed shear wall seismic design method, Thin-Walled Struct. 95 (2015) 48–59, http://dx.doi.org/10.1016/j.tws.2015.06.011.
[36] CEN, EN 1991-1-1 Eurocode 1: Actions on Structures-Part 1-1: General Actions-Densities, Self-weight, Imposed Loads for Buildings, European Committee for Standardization, Brussels, 2004.
[37] CEN, EN 1993-1-1 Eurocode 3: Design of Steel Structures-Part 1-1: General Rules and Rules for Buildings, European Committee for Standardization, Brussels, 2005.
[38] CEN, EN 1993-1-3 Eurocode 3: Design of Steel Structures-Part 1-3: General Rules-Supplementary Rules for Cold-Formed Members and Sheeting, European Committee

for Standardization, Brussels, 2006.
[39] CEN, EN 1998-1 Eurocode 8: Design of Structures for Earthquake Resistance-Part 1: General Rules, Seismic Actions and Rules for Buildings, European Committee for Standardization, Brussels, 2004.
[40] V. Macillo, S. Shakeel, L. Fiorino, R. Landolfo, Development and calibration of a hysteretic model for CFS strap braced stud walls, Int. J. Adv. Steel Constr. 14 (3) (2018) Sept.
[41] H. Krawinkler, P. Francisco, L. Ibarra, A. Ayoub, R. Medina, CUREE Publication No. W-02 Development of a Testing Protocol for Woodframe Structures, 2001.